

Regulation of membrane scission in yeast endocytosis

Deepikaa Menon¹ and Marko Kaksonen^{1*}

*For correspondence:

Marko.Kaksonen@unige.ch ()

¹Department of Biochemistry, University of Geneva, Geneva, Switzerland

Abstract

Introduction

Clathrin-mediated endocytosis (CME) is the major endocytic process by which cargo from the cell exterior is incorporated into a Clathrin-coated vesicle that is then transported into the cell interior (Bitsikas *et al.*, 2014). Over 50 different proteins are involved in reshaping a flat plasma membrane into an invagination that eventually forms the vesicle (Kaksonen and Roux (2018). Forces that drive the transition from invagination to spherical vesicle in multicellular eukaryotes are provided by the GTPase Dynamin (Grigliatti *et al.* (1973); Sweitzer and Hinshaw (1998); Ferguson *et al.* (2007); Takei *et al.* (1995); Galli *et al.* (2017). Dynamin is now known to interact via its proline-rich-domain with SH3 domains of crescent-shaped N-BAR proteins like Endophilin and Amphiphysin (Grabs *et al.* (1997); Cestra *et al.* (1999); Farsad *et al.* (2001); Ferguson *et al.* (2009); Meinecke *et al.* (2013). Conformation changes of Dynamin recruited to N-BAR molecules cause constriction of the underlying invaginated membrane, resulting in vesicle formation (Shupliakov *et al.* (1997); Zhang and Hinshaw (2001); Zhao *et al.* (2016).

In yeast, CME is the only pathway for uptake of cargo, and involves a similar membrane transformation as in other eukaryotes. Most mammalian CME proteins have homologues in yeast: these proteins drive the establishment of endocytic sites, form the mechanical link between membrane and actin proteins (Kaksonen and Roux (2018). Actin nucleation and polymerization drives the formation of tubular invaginations in yeast (Kübler *et al.*, 1993; Kaksonen *et al.*, 2003). The role of Dynamin in this process has been debated: yeast dynamin-like protein Vps1 has a major role in the Golgi and other membrane trafficking pathways (Rothman *et al.* (1990); Peters *et al.* (2004); Hoepfner *et al.* (2001), and been proposed to interact with endocytic proteins (Nannapaneni *et al.* (2010); Yu and Cai (2004); Smaczynska-de Rooij *et al.* (2012). Its contribution to CME is however, still debated (Goud Gadila *et al.* (2017); Kishimoto *et al.* (2011). In yeast cells, what causes membrane scission is thus unclear, although the yeast N-BAR Rvs complex (a heterodimeric complex of the proteins Rvs161 and Rvs167) has been identified as an important component of the scission module (Munn *et al.* (1995); Kaksonen *et al.* (2005); D'Hondt *et al.* (2000); Kishimoto *et al.* (2011). The two Rvs proteins are homologues of N-BAR proteins Amphiphysin and Endophilin (Friesen *et al.* (2006); Youn *et al.* (2010). Deletion of Rvs167 reduces scission efficiency by nearly 30% and reduces the invagination lengths at which scission occurs (Kaksonen *et al.* (2005); Kukulski *et al.* (2012). Apart from the canonical N-BAR domain which forms the crescent-shaped structure, Rvs167 has a Glycine-Proline-Alanine rich (GPA) region and a C-terminal SH3 domain (Sivadon *et al.* (1997). The GPA region is thought to act as a linker with no other known function, while loss of the SH3 domain affects budding pattern and actin morphology (Sivadon *et al.* (1997). Most Rvs deletion phenotypes

43 can be rescued by expression of the BAR domains alone *Sivadon et al. (1997)*, suggesting that the
44 BAR domains are the functional unit of the Rvs complex.

45 The Rvs complex can tubulate liposomes in vitro, indicating that the BAR domains can impose
46 curvature on membranes *Youn et al. (2010)*. However, Rvs arrives at endocytic sites when mem-
47 brane tubes are already formed: curvature sensing rather than generation is the likely interaction
48 of the complex with endocytic sites *Kukulski et al. (2012)*; *Picco et al. (2015)*. Rvs molecules arrive
49 at endocytic sites about 4 seconds before scission, and disassemble rapidly at the time of scission
50 *Picco et al. (2015)*, consistent with a role in scission. While it is shown to be involved in the last
51 stages of endocytosis, a mechanistic understanding of the influence of Rvs on scission remains
52 incomplete.

53
54 Several scission models have been proposed that allow a major role for Rvs and are tested in this
55 work. Although the yeast Dynamin Vps1 lacks a canonical BAR-protein binding site *Bui et al. (2012)*;
56 *Moustaq et al. (2016)*, it may be recruited via a different mechanism and induce scission. Liu et
57 al., proposed that Synaptojanins may selectively hydrolyze lipids at endocytic sites, causing line
58 tension between two lipid types that results in scission *Liu et al. (2009)*. Protein friction along the
59 membrane invagination has been proposed as a mechanism by which scission may occur

60 Simunovic2017b. We used quantitative live-cell imaging and genetic manipulation in *Saccha-*
61 *romyces cerevisiae* to test these theories and investigate the function of Rvs in endocytosis. We
62 found that Rvs is recruited to endocytic sites by both BAR and SH3 domains. Of several potential
63 actin-interacting binding partners of the SH3 domains such as Myo3, Myo5, Vrp1, Abp1 *Lila and Dru-*
64 *bin (1997)*; *Colwill et al. (1999)*; *Madania et al. (1999)*; *Liu et al. (2009)*. we found that type I myosin
65 Myo3 interacts with Rvs SH3 domains. Our data also suggests that the aforementioned theories
66 of membrane scission are unlikely to sever the membrane in yeast, and that actin polymerization
67 likely generates the forces required for scission.

68 Results

69 Rvs167, rather than Vps1 influences coat movement

70 Yeast Dynamin-like protein Vps1 does not contain a Proline Rich Domain, which in mammalian
71 cells is required for recruitment to endocytic sites *Grabs et al. (1997)*; *Cestra et al. (1999)*; *Farsad*
72 *et al. (2001)*; *Meinecke et al. (2013)*. In spite of the lack of a stereotypical interaction domain, some
73 works have reported its recruitment to endocytic proteins, including to N-BAR protein Rvs167 *Yu*
74 *and Cai (2004)*; *Nannapaneni et al. (2010)*; *Rooij et al. (2010)*. The question of whether or not Vps1
75 has a function at endocytic sites has been obfuscated by potential tagging-induced dysfunction
76 of Vps1 molecules. Vps1 tagged both N- and C-terminally with GFP constructs failed to co-localize
77 with endocytic protein Abp1 in our hands, consistent with other work that observed localization
78 only with other parts of the trafficking pathway *Goud Gadila et al. (2017)*. We argued that even
79 if tagging Vps1 induced defects in its localization and/or function, its contribution to endocytosis
80 could be examined by observing the dynamics of other endocytic proteins in cells lacking Vps1. The
81 canonical interaction partner of Vps1- Rvs167- localizes to endocytic sites, and has a role in scission,
82 although it is unclear what that is *Kukulski et al. (2012)*; *Picco et al. (2015)*. In order to determine
83 the roles of these proteins in endocytic scission, we studied cells lacking Vps1 and Rvs167, and
84 compared against wild-type (WT) cells (Fig.1A-F).

85
86 Vps1 deletion was confirmed by sequencing the gene locus, and these cells showed a previously
87 reported ? growth phenotype at 37°C (Fig.1, supplement1). Scission efficiency was quantified
88 by tracking the endocytic coat protein Sla1 tagged at the C-terminus with eGFP (Fig.1C). Upon
89 actin polymerization, the endocytic coat moves into the cytoplasm along with the membrane as
90 it invaginates (Skrzyny et al. 2012). Movement of coat protein Sla1 thus acts as a proxy for the
91 growth of the plasma membrane invagination. Membrane retraction, that is, inward movement and

subsequent retraction of the invaginated membrane back towards the cell wall is a scission-specific phenotype *Kaksonen et al. (2005)*. Retraction rates do not significantly increase in *vps1Δ* cells compared to the WT (Fig.1C).

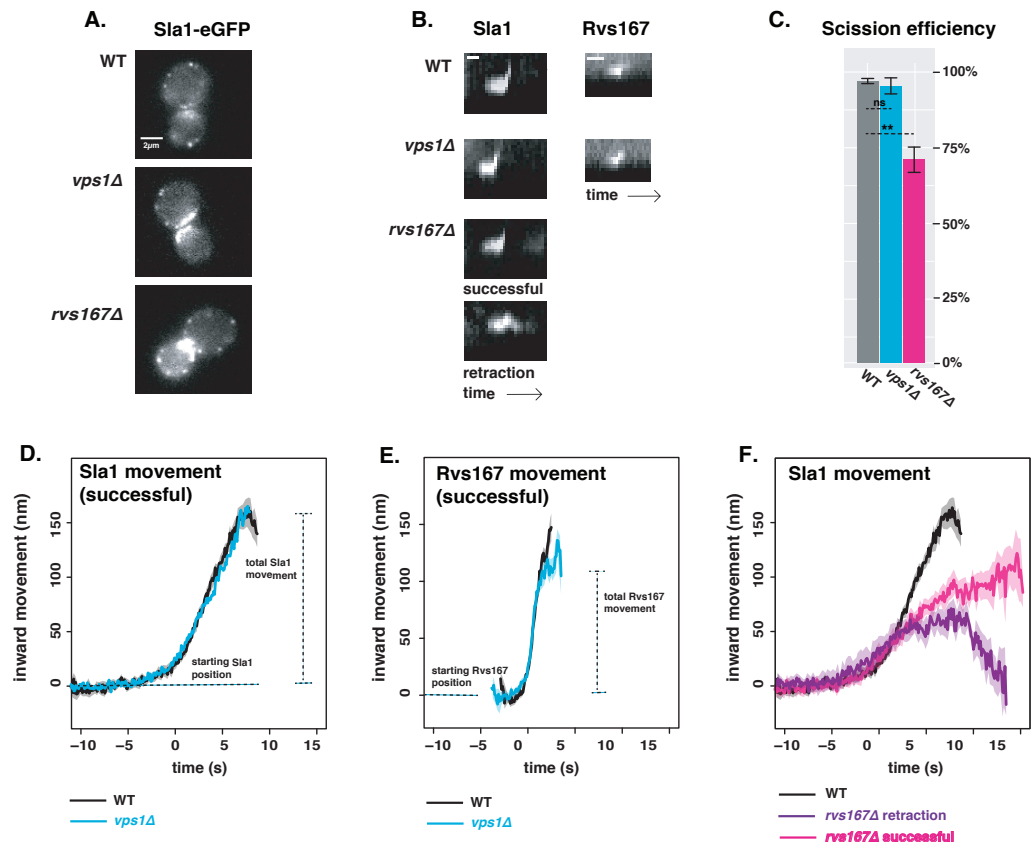


Figure 1. *vps1Δ* and *rvs167Δ* deletion **A:** Slice from image of WT, *vps1Δ*, and *rvs167Δ* cells expressing Sla1-eGFP. Scale bar= 2μm. **B:** Representative kymographs of Sla1-eGFP and Rvs167-eGFP patches in WT, *vps1Δ*, and *rvs167Δ* cells. Scale bar for Sla1-egfp = 20(s), scale bar for Rvs167-eGFP = 5(s). **C:** Histogram of Sla1-eGFP retraction percentages in WT, *vps1Δ*, and *rvs167Δ* cells. Error bars are standard deviation from two data sets, $p < 0.001 = *$. **D:** Averaged centroid positions of Sla1-eGFP in WT and *vps1Δ* cells. **E:** Averaged position of Rvs167-eGFP in WT and *vps1Δ* cells. **F:** Averaged position of Sla1-eGFP in WT, and successful and retracted Sla1-eGFP positions in *rvs167Δ* cells. All averaged positions are aligned in time to begin inward movement at the same time=0(s), and aligned in space to a starting position = 0(nm). Note that in E, averaged Rvs167-eGFP inward movement is concomitant with the maxima of its fluorescent intensity (Fig1.supplement3)

In order to study the total inward movement of the endocytic coat, and therefore the depth of the endocytic invagination, the averaged centroid trajectory of 50 Sla1-eGFP patches (ref. Picco, eLife 2015) in *vps1Δ* and WT cells is tracked and compared (Fig.1D). In brief: yeast cells expressing fluorescently-tagged endocytic proteins are imaged at the equatorial plane. Since membrane invagination progresses perpendicularly to the plane of the plasma membrane, proteins that move into the cytoplasm during invagination do so in the imaging plane. Centroids of Sla1 patches- each patch being an endocytic site- are tracked in time and averaged. This provides an average centroid that can be followed with high spatial and temporal precision. For more details, refer to Picco et. al, eLife 2015. Averaged centroid movement of Sla1-eGFP in WT cells is linear to about 140nm (Fig.1D). Sla1 movement in *vps1Δ* cells has the same magnitude of movement (Fig.1D). In spite of slight

differences in the rates of movement, the total inward movement- and so the depth of endocytic invagination- does not change.

Centroid tracking has shown that the number of molecules of Rvs167 peaks at the time of scission, and is followed by a rapid loss of fluorescent intensity, simultaneous with a sharp jump of the centroid into the cytoplasm (ref.Andrea). This jump, also seen in Rvs167-GFP kymographs (Fig.1B), is interpreted as loss of protein on the membrane tube, causing an apparent spatial jump to the protein localized at the base of the newly formed vesicle. Kymographs of Rvs167-GFP (Fig.1B), as well as Rvs167 centroid tracking (Fig.1E) in Vps1 deleted cells show the same jump as in WT.

Since removal of the Rvs complex is known to increase the membrane retraction rate at endocytic sites (ref Marko), involvement of the Rvs proteins in the scission process was investigated further. The Rvs complex is composed of Rvs161 and Rvs167 dimers (ref.Dominik), so deletion of Rvs167 effectively removes both proteins from endocytic sites. We quantified the effect of *rvs167Δ* on membrane invagination (Fig.1A-C). 27% of Sla1 patches move inward and then retract in *rvs167Δ* cells (Fig.1C). Similar retraction rates were measured in other experiments (Kaksonen, Toret and Drubin, 2005), and suggest failed scission in these 27% of endocytic events. Coat movement both of retractions and of successful endocytic events were quantified (Fig.1F) as described in Picco et. al, 2015. Sla1 centroid movement in both successful and retracting endocytic events in *rvs167Δ* cells look similar to WT up to about 50nm (Fig.1F). In WT cells, Abp1 intensity begins to drop at scission time; similarly, in successful endocytic events, Abp1 intensity drops after Sla1 centroid has moved about 100nm (Fig.1supplement), suggesting that scission occurs at invagination lengths between 60 -100 nm. That membrane scission occurs at shorter invagination lengths than in WT is corroborated by the smaller vesicles formed in *rvs167Δ* cells by Correlative light and electron microscopy (CLEM) (Kukulski et al., 2012). CLEM has moreover shown that Rvs167 localizes to endocytic sites after the invaginations are about 60nm long (Kukulski et al., 2012). Sla1 movement in *rvs167Δ* indicates therefore that membrane invagination is unaffected till Rvs is supposed to arrive. The Sla1 centroid for retraction events moves back towards its original position after inward movement.

Synaptojanins likely influence vesicle uncoating, but not scission dynamics.

Three Synaptojanin-like proteins have been identified in budding yeast: Inp51, Inp52, and Inp53. Inp51-eGFP exhibits a diffuse cytoplasmic signal, Inp52-eGFP localizes to cortical actin patches that are endocytic sites (Fig2 supplement) and Inp53 localizes to patches within the cytoplasm (ref). Spatial and temporal alignment of Inp52 with Sla1, Abp1, and Rvs167 (ref.Pico) shows that Inp52 protein molecules arrive in the late stage of endocytosis after Rvs167, and localizes to the invagination tip, suggesting a potential role in membrane scission (Fig.2b).

Inp53 was not investigated further, as its localisation conforms with other literature that find it is involved in the golgi trafficking pathway rather than endocytosis (ref Golgi). Although we were unable to see Inp51 localisation at endocytic sites, it may be recruited in small numbers below our detection limit. Deletion of Inp51 has been shown to exacerbate the effect of *inp52Δ* on membrane retraction (ref Liu), so both Inp51 and Inp52 were tested as potential candidates as scission regulators.

Dynamics of Sla1-eGFP and Rvs167-eGFP in either *inp51Δ* or *inp52Δ* cells were compared against the WT. Membrane retraction events do not significantly increase in either compared to the WT (Fig2c).

Magnitude and speed of Sla1 and Rvs167 centroid movement in *inp51Δ* is the same as the WT (Fig2.d, e). In *inp52Δ* cells, Sla1 movement also has the magnitude and speed as WT, but Sla1-eGFP signal is persistent after membrane scission (Fig.2d, arrow). Similarly, although Rvs167 inward

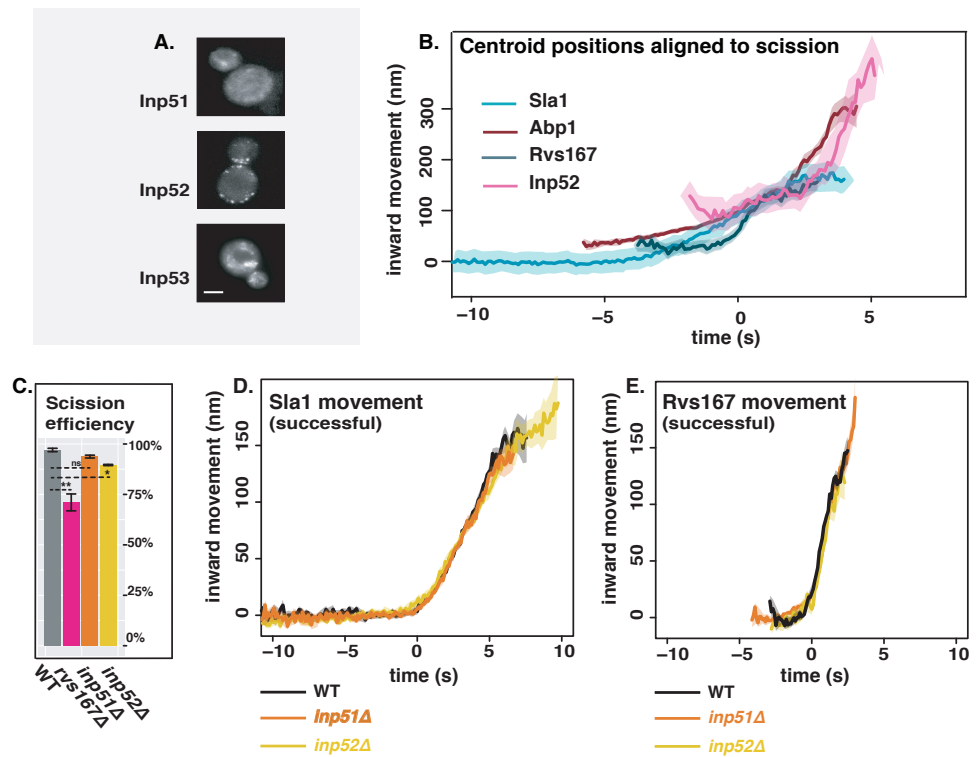


Figure 2. Involvement of yeast Synaptojanin-like proteins in endocytosis A. Cells with endogenously tagged Inp51, Inp52, and Inp53. B. Inp52 centroid trajectory is aligned in space and time to other endocytic proteins. C: Sla1 retraction rates in *inp51Δ* and *inp52Δ* cells compared to WT and *rvs167Δ*. Error bars are standard deviation from two data sets. D: Averaged centroid positions of Sla1-eGFP in WT, *inp51Δ*, and *inp52Δ* cells. E: Averaged centroid positions of Rvs167-eGFP in WT, *inp51Δ*, and *inp52Δ* cells.

157 movement looks similar to WT in *inp52Δ* (Fig2e), Rvs167-eGFP signal is persistent after inward
 158 movement (Fig2e arrow), and Rvs167 and Sla1 disassembly has a delay (Fig2 supplement)

159 **Rvs BAR domains recognize membrane curvature in-vivo**

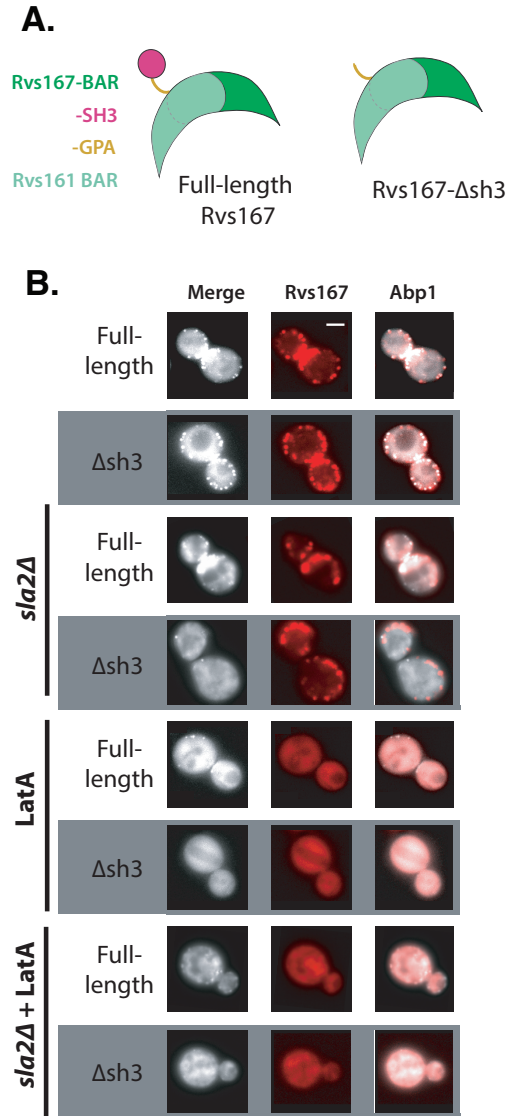


Figure 3. Localization of Rvs167 BAR domain A: Schematic of Rvs protein complex with and without the SH3 domain. B: Localization of full-length and BAR-GPA in WT, *sla2Δ*, LatA treated, and LatA treated *sla2Δ* cells. C: Localization of full-length Rvs167-eGFP in WT, *myo3Δ*, *myo5Δ*, and *vrp1Δ* cells. Scale bars=2μm.

160 So far Rvs167 remains the protein that has a major influence on scission rates and inward
 161 moment of Sla1. Recruitment of the Rvs complex to endocytic sites was thus investigated further.
 162 Interaction between Rvs and membrane curvature in vivo has been indicated by work on other BAR
 163 domain proteins (ref BAR), but has not so far been tested. In order to do so, we deleted the SH3
 164 domain of Rvs167 leaving the N-terminal BAR and GPA regions (henceforth BAR-GPA, Fig3a) and
 165 observed the localization of the BAR region without SH3 influence. The GPA region is a disordered
 166 domain that has no previously reported function (ref) and was retained to ensure proper folding and
 167 function of the BAR domain. Endogenously tagged Rvs167-eGFP and BAR-GPA-eGFP colocalization

168 with Abp1-mCherry in WT and *sla2Δ* cells were compared (Fig3b). Sla2 acts as the molecular linker
 169 between forces exerted by the actin network and the plasma membrane (ref. Skruzny). *sla2Δ* cells
 170 therefore contain a polymerizing actin network at endocytic patches, but the membrane has no
 171 curvature, and endocytosis fails. In these cells, the full-length Rvs167 protein co-localizes with
 172 Abp1-mCherry, indicating that it is recruited to endocytic sites (Fig3b, "*sla2Δ*"). BAR-GPA localization
 173 is removed, except for rare transient patches that do not co-localize with Abp1-mCherry.

174 **Rvs SH3 domains have an actin and curvature independent localisation**

175 The SH3 domain has known genetic interactions with actin-related endocytic proteins. In order to
 176 test if these interactions are prevalent in vivo, we tested the localisation of full-length Rvs167 and
 177 BAR-GPA in LatA treated cells (Fig3b, "LatA"). Plasma membrane localisation of full-length Rvs167
 178 remains upon LatA treatment, and transient patches continue to exist in *sla2Δ* cells treated with
 179 LatA (Fig3b, "*sla2Δ*+ LatA"). BAR-GPA localisation on the other hand, is removed in both.

180 **SH3 domains are likely recruited by Myosin 3**

181 Type I myosins Myo3 and Myo5, and Vrp1 have genetic or physical interactions with Rvs167 SH3
 182 domains (Lila and Drubin, 1997; Colwill et al., 1999, Madania et al., 1999; Liu et al., 2009). We tested
 183 the interaction between these proteins and the Rvs167 SH3 region by studying the localization
 184 of full-length Rvs167 in cells with one of these proteins deleted, and treated with LatA. By LatA
 185 treatment we expected to produce the situation in which BAR-curvature interaction is removed
 186 (Fig3b). Then if we lost SH3 interaction because we deleted the protein with which it interacts, we
 187 would lose localisation of Rvs167 completely. Deletion of neither Vrp1 nor Myo5 in combination
 188 with LatA treatment removes the localization of Rvs167. Deletion of Myo3 with LatA treatment
 189 removes localization of Rvs167.

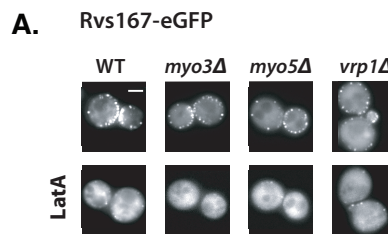


Figure 4. Localization of the SH3 domain A: Schematic of Rvs protein complex with and without the SH3 domain, roughly based on homology models with Amphiphysin and Endophilin. B: Localization of full-length and BAR-GPA in WT, *sla2Δ*, LatA treated, and LatA treated *sla2Δ* cells. C: Localization of full-length Rvs167-eGFP in WT, *myo3Δ*, *myo5Δ*, and *vrp1Δ* cells. Scale bars=2μm.

190 what about the differences in myo5 and myo3 number...

191 **Loss of Rvs167 SH3 domain affects coat and actin dynamics**

192 Since the Rvs167 SH3 domain appears to have an important influence on the recruitment of the
 193 Rvs complex to endocytic sites, we wondered if the domain also had an influence on endocytic
 194 dynamics. We compared dynamics of Sla1 and Rvs167 in WT and BAR-GPA strains (Fig4). Movement
 195 of Sla1 centroid is slower in BAR-GPA cells than in WT (Fig4a). Tubular invaginations are formed
 196 in BAR-GPA cells, and qualitatively resemble those in WT, as seen by CLEM (Fig.4 supplement).
 197 Recruitment of both Rvs167 and Abp1 molecules is delayed in BAR-GPA cells. However, Rvs167
 198 centroids in both WT and BAR-GPA arrive at endocytic sites when the Sla1 centroid is 20-30 nm
 199 away from its starting position. BAR-GPA accumulation also begins when Abp1 molecule numbers
 200 in the mutant are about the same as in WT (about 300 copies, Fig4b). Taken together, this data
 201 suggests that the Rvs complex is recruited to a specific geometry of membrane invagination, and

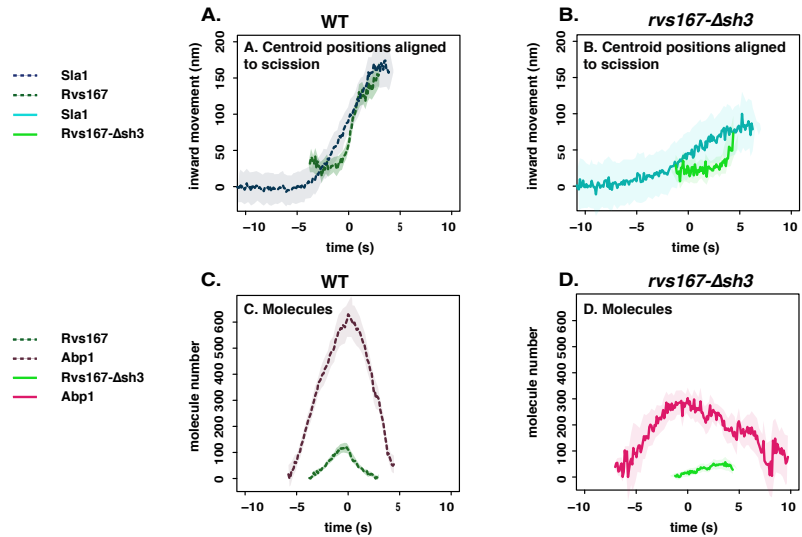


Figure 5. Endocytic dynamics in BAR-GPA cells A: Averaged centroid positions of Sla1 and Rvs167 aligned in space and time so that time=0(s) is the peak of fluorescent intensity of Abp1 in WT and BAR-GFP strains. B: Numbers of molecules of in WT and BAR-GPA strains, aligned so that time=0(s) is the maximum of fluorescent intensity of Abp1 in the corresponding strains.

that Rvs167 recruitment in BAR-GPA is delayed because invaginations in this mutant take longer to acquire this specific geometry.

The inward jump of Rvs167 is smaller in BAR-GPA cells than in WT (Fig.4b), consistent with the formation of shorter invaginations suggested by the reduced Sla1 movement in these cells. Recruitment of Rvs167 in BAR-GPA cells is reduced to half of that in WT (Fig.4b), although cytoplasmic concentration of Rvs167 in both cell types are not different (Fig.4 supplement). Recruitment therefore is unlikely to be limited by cytoplasmic expression of the mutant protein. Abp1 disassembly is slowed down in BAR-GPA cells compared to WT, and recruitment is reduced to 50% of WT recruitment (Fig.4b), likely indication disruption of actin network dynamics.

Increased BAR domain recruitment corresponds to increased membrane movement

We wondered if the decreased Sla1 movement in BAR-GPA cells (Fig.4a) was induced by loss of an SH3 domain mediated interaction, or because Rvs167 in the BAR-GPA mutant is recruited in smaller numbers to endocytic sites. To check whether increasing the recruitment of the Rvs complex can rescue reduced Sla1 movement, Rvs167 and Rvs161 genes were duplicated endogenously (ref Huber) in diploid and haploid yeast cells. In haploid cells, increasing the number of Rvs167 and Rvs161 genes results in increased recruitment of Rvs167 to about 1.6 times the WT amount (Fig.5c). Sla1 dynamics remains the same as in the WT (Fig.5a). Duplicating the BAR-GPA domain alone increases the amount of BAR-GPA molecules recruited to endocytic sites (Fig.5c), and rescues the loss of Sla1 movement in the 1x BAR-GPA, as well the inward jump of BAR-GPA itself (Fig.5a,b). By gene duplication, diploid cells are generated containing either 4 copies of both Rvs genes, 2 copies of each gene (WT diploid), or 1 copy (by deleting one copy of Rvs167 and Rvs161). In diploid cells (Fig.5d-f), amount of Rvs167 recruited to sites increases with gene copy number (Fig.5f). Adding excess Rvs to endocytic sites in the 4x case does not change the rate or total inward movement of Sla1, or of Rvs167 (Fig.5d,e). In the case of 1x Rvs, Sla1 movement is slightly reduced after 100nm (Fig.5a). Magnitude of Rvs167 inward movement is unchanged, but the Rvs167-eGFP signal is lost immediately after the inward movement, unlike in the 4x and 2x cases. We measured the total number of Abp1 molecules at endocytic sites for different strains (Fig.5g,h), and found that higher

230 Abp1 numbers corresponds to larger Sla1 centroid movement. Total Abp1 numbers recruited are
 231 reduced for 1xBAR and *rvs167Δ* strains (Fig5g,h), suggesting a correlation between the maximum
 232 number of Abp1 recruited and total invagination length.

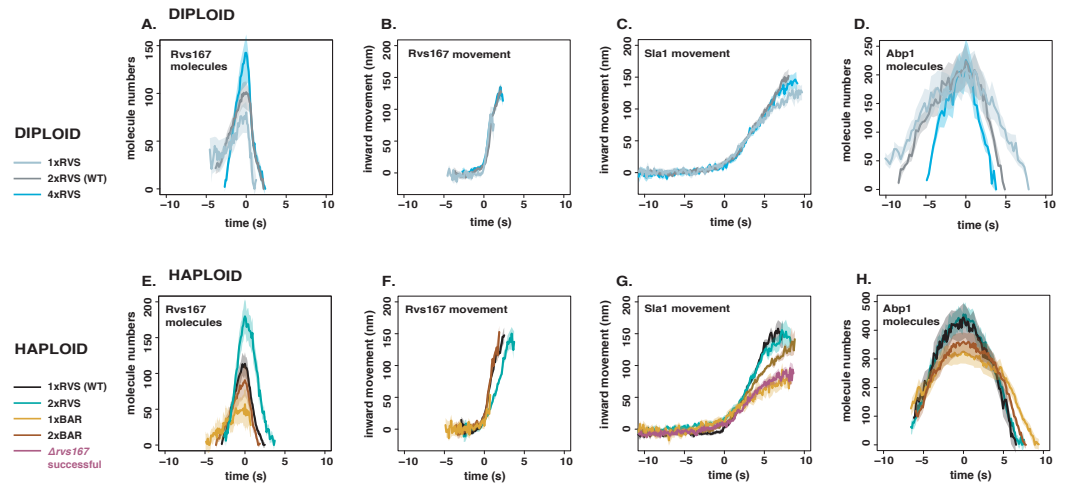


Figure 6. RVS duplication in haploid and diploid cells A: Sla1 centroid positions in haploid strains with different numbers of copies of Rvs167 and Rvs161 genes. B: Rvs167 centroid positions. C: Recruitment of Rvs167 in time in these strains. D: Sla1 centroid positions in diploid strains expressing different numbers of copies of Rvs167 and Rvs161. E, F: Rvs167 centroid positions, and recruitment in time, in the diploid strains. All centroid positions are aligned in the time axis so that time=0(s) corresponds to beginning of inward movement of the average centroid for each corresponding strain. They are aligned in the y axis so that y=0(nm) corresponds to the beginning of the average centroid position

233 Discussion

234 Recruitment and function of the Rvs complex in has been explored in this work, as well as several
 235 models for how membrane scission could be effected in yeast endocytosis. We propose that
 236 Rvs is recruited to endocytic sites by interactions between the Rvs BAR domains and invaginated
 237 membrane, and that SH3 domain mediated protein-protein interactions are required for efficient
 238 recruitment of Rvs to sites. Arrival of Rvs on membrane tube scaffolds the membrane and prevents
 239 premature membrane scission. Effective scaffolding depends on recruitment of a critical number
 240 of Rvs molecules. Rvs is a relatively short-lived protein at endocytic sites. It is recruited only once
 241 membrane tube is formed (Kaksonen, Toret and Drubin, 2005; Kukulski et al., 2012; Picco et al.,
 242 2015). FCS measurements (Boeke et al., 2014) have shown that the cytosolic concentrations of
 243 Rvs167 and Rvs161 are high (354nM and 721nM respectively) compared to other endocytic proteins
 244 like Las17, Vrp1, Myo3, and Myo5 (80-240nM). In spite of this, relatively few numbers of Rvs are
 245 recruited to endocytic sites, suggesting that recruitment is tightly regulated. In the case of Rvs, both
 246 timing and efficiency appear crucial to its function, the question is what confers both.

247 BAR domains sense *in vivo* membrane curvature and time recruitment of Rvs

248 The curved structure of BAR dimers (Peter et al., 2004; Mim et al., 2012) has suggested that Rvs
 249 is recruited by its preference for some membrane shapes over others, supported by its arrival at
 250 curved membrane tubes. In the absence of membrane curvature, in *sla2Δ* cells, the BAR domain
 251 alone does not localize to cortical patches (Fig.3b,c). This demonstrates for the first time that the
 252 BAR domain does indeed sense and requires membrane curvature to localize to cortical patches.
 253 Work on BAR domains have proposed that electrostatic interactions at the concave surface and
 254 tips of the BAR domain structure mediate membrane binding (Qualmann, Koch and Kessels, 2011).

255 Mutations in these lipid-binding surfaces would clarify the interaction with underlying lipids, and
 256 test if Rvs relies on similar interactions. BAR is able to localize to endocytic sites, and has a similar
 257 lifetime in WT cells (Fig4b). However, time alignment with Abp1 shows that there is a delay in the
 258 recruitment of BAR-GPA compared to Abp1 arrival, compared to full-length Rvd167 (Fig4c). The
 259 delayed recruitment occurs because the invagination takes longer to reach a particular length: Sla1
 260 moves inwards at a slower rate in BAR cells, and it takes longer for the membrane in BAR-GPA cells
 261 to reach the same length as Rvs167. Rvs167 arrives in BAR cells when Sla1 has moved inwards
 262 25-30nm (dashed red lines in Fig.4a), which is also the distance Sla1 has moved when Rvs167 arrives
 263 in WT. By the time Sla1 has moved this distance, the membrane is already tubular (Kukulski et
 264 al., 2012; Picco et al., 2015), consistent with Rvs arrival at invaginated tubes. This suggests Rvs
 265 recruitment is timed to specific membrane invagination length- therefore to a specific membrane
 266 curvature- and that this timing is provided by the BAR domain.

267 **SH3 domains allow efficient and actin independent recruitment**

268 Rvs167 in BAR cells accumulates to about half the WT number (Fig.3c), even though the same cyto-
 269 plasmic concentration is measured (supplement Fig3?), indicating that the SH3 domain increases
 270 the efficiency of recruitment of Rvs. In *sla2Δ* cells, full-length Rvs can assemble on the membrane
 271 (Fig.3b,c). Since BAR domains alone do not localize to patches in *sla2Δ* cells, full-length localiza-
 272 tion must be mediated by the SH3 domain, supporting a role for the SH3 domain in increasing
 273 recruitment of Rvs by clustering protein molecules. That full-length Rvs167 is able to assemble and
 274 disassemble at cortical patches in *sla2Δ* cells without the curvature- dependent interaction of the
 275 BAR domain (Fig.3b,c) indicates that the SH3 domain is able to mediate both the recruitment and
 276 the disassembly of Rvs at the endocytic site. In *sla2Δ* cells treated with LatA (Fig.3c), actin-based
 277 membrane curvature is inhibited, and the actin patch proteins are removed from the plasma mem-
 278 brane. Full-length Rvs167 in these cells still shows transient localizations at the plasma membrane.
 279 In *sla2Δ* cells treated with LatA, the localization of BAR is lost. This suggests that localization of the
 280 full-length Rvs167 in LatA treated cells is dependent on an SH3 domain interaction, and that this is
 281 independent of both actin and membrane curvature.

282 In WT cells, the Abp1 and Rvs167 fluorescent intensities reach maxima concomitantly (Fig4b),
 283 and the consequent decay of both also coincide. Coincident disassembly indicates that upon vesicle
 284 scission, the actin network is immediately disassembled. Membrane scission essentially occurs
 285 around the intensity peak of the two proteins. This coincident peak is lost in BAR-GPA cells: BAR-
 286 GPA-eGFP in these cells peaks several seconds after Abp1 intensity starts to drop, and the decay of
 287 Abp1 is prolonged, taking nearly double the time as in WT. The number of Abp1 molecules recruited
 288 is decreased to about two thirds the WT number. Although it is not clear what the decoupling of
 289 Abp1 and Rvs peaks means, the changes in Abp1 dynamics suggests a strong disruption of the actin
 290 network dynamics. SH3 domains are known to interact with components of the actin network like
 291 Abp1 and Las17 (Lila and Drubin, 1997, Madania et al., 1999), but study of other components of
 292 the actin machinery will be required to understand how exactly loss of the SH3 has changed the
 293 progression of endocytosis.

294 SH3 interaction with an endocytic binding partner likely help recruit Rvs to endocytic sites. Many
 295 such interaction partners have been proposed. Abp1 interaction with the Rvs167 SH3 domain
 296 has been shown (Lila and Drubin, 1997; Colwill et al., 1999), as has one with WASP protein Las17
 297 (Madania et al., 1999; Liu et al., 2009), yeast Calmodulin Cmd1 (Myers et al., 2016), type I myosins
 298 (Geli et al., 2000), and Vrp1 (Lila and Drubin, 1997). All of these suggested binding partners localize
 299 to the base of the invagination (Yidi Sun, 2006; Picco et al., 2015), and do not follow the invaginating
 300 membrane into the cytoplasm. The SH3 interaction partner is likely Myo3 (Fig3d), and SH3 domains
 301 interact with the endocytic network at the base of the invagination. Centroid tracking however,
 302 suggests that Rvs is accumulated all over the membrane tube. If Rvs was recruited to the base and
 303 pulled up as the invagination grows, the centroid would move continuously upwards rather than
 304 remain relatively non-motile before the jump at scission time. It is possible that the SH3 initially

305 helps cluster near the base, and as the membrane invaginations grow longer, BAR-membrane
306 interactions dominate.

307 **Accumulation of Rvs on membrane invagination**

308 When ploidy is doubled from haploid to diploid yeast cells, we could expect that double the protein
309 amount is expressed and recruited, but it does not appear so. The amount of Rvs recruited in
310 WT haploid and diploids remains about the same, and cytoplasmic signal is similar (Fig.5, Fig5
311 supplement). This invariance between accumulated protein in haploids and diploids shows that Rvs
312 recruitment is not determined by the number of alleles of Rvs. Haploid and diploid cells appear
313 to tune the amount of Rvs recruitment to get a specific amount to endocytic sites. WT diploids
314 (2xd) contain two copies each of RVS161 and RVS167 genes. Rvs duplicated diploids, which contain
315 four copies each of RVS167 and RVS161 (4xd) could be expected to express and recruit to sites
316 twice the amount of Rvs as 2xd. However, compared to 2xd, cytoplasmic signal in 4xd increases
317 by 1.6x and recruitment of Rvs167 to endocytic sites increases only by 1.4x. Doubling the gene
318 copy number increases, but does not double protein expression or recruitment in the case of
319 Rvs. Similarly, duplicating Rvs genes in haploid cells results in an increase in number of molecules
320 recruited, but not in doubling (1xh, 2xh). Although the rate of adding Rvs is different in haploids and
321 diploids, in both cases, it increases by gene copy number (yellow line in Fig.4.2). Cytoplasmic protein
322 concentration is increased when gene copy number is increased, and recruitment to endocytic
323 sites is increased by the increase in cytoplasmic concentration. These data suggest that the amount
324 of Rvs that is recruited scales with available concentration of protein. Comparing across ploidy
325 however, the rate of Rvs recruitment is lower in WT diploid compared to WT haploid (2xd vs 1xh,
326 Fig.4.1)

327 for this is not clear. 4.2 Arrangement of Rvs dimers on the membrane A homology model of
328 the Rvs BAR dimer structure based on Am- phiphysin suggests that it has the concave structure
329 typical for N- BAR domains. Rvs is a hetero- rather than homodimer unlike Am- phiphysin, and a
330 high-resolution structure will be necessary to clarify the interaction and arrangement of Rvs on
331 endocytic tubes. There are some indications from the experiments in this thesis however, regarding
332 its interaction with the membrane. 4.2.1 Rvs does not form a tight scaffold on membrane tubes
333 Observations of in vitro helices of BAR domains have suggested that Rvs might form a similar helical
334 scaffold. The number of Rvs molecules recruited to endocytic sites is high enough to cover the
335 surface area of the tubular invagination, so it has been proposed that an Rvs scaffold covers the
336 entire membrane tube up to the base of the future vesicle (Picco et al., 2015). In Rvs duplicated
337 diploid cells (4xd), Rvs can be recruited at a much faster rate than in the WT (2xd) (Fig.3.10B-
338 C, Fig.4.2) while disassembly dynamics is the same in both (Fig.3.10C, Fig.4.3). The exponential
339 decay of fluorescent intensity in WT haploid and diploid cells (1xh, 2xd, Fig.4.3) indicates that
340 all of the protein is suddenly disassembled from the endocytic site. When the membrane tube
341 undergoes scission, there is no more tubular curvature for the Rvs to bind to. The sharp decay is
342 therefore consistent with a BAR scaffold that breaks upon vesicle scission because there is no more
343 membrane interaction, releasing all the membrane-bound protein at once. A similar decay in the
344 4xd strain suggests that all the Rvs in this case is also bound to the membrane: if the protein was
345 not bound to the membrane, fluorescent intensity would not decay sharply. Since the membrane is
346 able to accommodate 1.4x the amount of BAR protein as the WT, it would suggest that at lower
347 protein amounts, a tight helix that covers the entire tube is not likely. Adding molecules to a tube
348 already completely covered by a scaffold would result in a change in Rvs assembly and disassembly
349 dynamics. Further, additional molecules would have to be added at the top or base of a tight
350 scaffold. At the top, the radius of curvature is decreased compared to the tube since this is the
351 rounded vesicle region. At the base, the plasma membrane is nearly flat, and the Rvs BAR domain
352 is similarly unlikely to favour interactions here. Otherwise the scaffold would have to be disrupted
353 to add new molecules, which would likely slow down recruitment rate rather than speed it up.
354 Molecules could also be added concentric to an existing scaffold. However, the concave surface of

Rvs is known to interact with lipids, and multiple layers of BAR domains on the membrane tube would probably not show the sudden disassembly seen here. I assume that the membrane surface area does not change in the 4xd compared to 2xd from the identical movement of Sla1 in both cases (Fig.3.10A). It is possible that a wider tube is formed, which would increase the membrane surface area for BAR binding. This would, however, require the BAR domains to interact with a lower radius of curvature than in WT. This seems unlikely, and in the absence of any indication otherwise, I assume that the membrane tubes in all diploid and haploid cases have the same width. 4.2.2 A limit for how much Rvs can be recruited to the membrane In the case of Rvs duplication in haploids (2xh), a change in disassembly dynamics is seen (Fig.3.9C, Fig.4.3). In 2xh, the maximum number of molecules recruited is 178 ± 7.5 compared to the maximum of 113.505 ± 5.2 in WT (1xh). This means that nearly 1.6x the WT amount of protein is recruited to membrane tubes in the 2xh case. The Rvs167 fluorescent intensity in 2xh shows a delay in disassembly. This suggests that the excess protein may not be directly on the membrane, since if the protein was membrane bound, when the membrane breaks, the protein must be released. The excess Rvs could either interact with the actin network via the SH3 domain, or interact with other Rvs dimers. By a similar argument as in 4.2.1 above, I do not expect that multiple layers of BAR domains are formed, and that the excess protein is recruited by the interaction of the SH3 domain. Another explanation for the delayed disassembly is that at high concentrations of Rvs like in the 2xh case, a tight BAR scaffold is formed, and the BAR domains interact with adjacent BAR domains. When the membrane undergoes scission, the protein is no longer membrane-bound, but lateral interactions delay disassembly of the scaffold. Lateral interactions between neighbouring BAR dimers have been shown in the case of Endophilin (Mim et al., 2012). It is not currently clear where the Rvs molecules are added in the 2xh case: superresolution microscopy could clarify whether it is added at the membrane tube. Whatever the arrangement of the Rvs complex on the membrane, disassembly dynamics is changed in the case of 2xh, compared to the other haploid and diploid strains. Since the number of Rvs molecules is highest in this strain, this suggests that there is a limit to how much Rvs can assemble on the tube without altering interaction with the endocytic protein network. 4.2.3 Conclusions for Rvs localization All of these data support the idea that Rvs recruitment rate and total numbers are determined by concentration of protein in the cell. The maximum number of molecules that can interact with the membrane is limited by the surface area of the invagination. Although more can be recruited, Rvs molecules over a certain threshold interact in a different way with endocytic sites, possibly via the SH3 domain. Timing of recruitment to sites is by curvature-recognition via the BAR domain, while efficiency of recruitment and interaction with the actin network is established via the SH3 domain. 4.3 What causes membrane scission?

Rvs acts as a membrane scaffold preventing membrane scission

Invaginations in *rvs167Δ* cells undergo scission at short invagination lengths of about 80nm (Fig.3.2), compared to the WT lengths of 140nm. This shows that first, enough forces are generated at 80nm to cause scission. Then, that Rvs167 is required at membrane tubes to prevent premature scission. Prevention of scission at short invagination lengths can be explained by Rvs stabilizing the membrane invagination via membrane interactions of the BAR domain (Boucrot et al., 2012; Dmitrieff and Nedelec, 2015). Rvs preventing membrane scission could also be explained by the SH3 domain mediating actin forces to the invagination neck: one can imagine that the SH3 domain somehow decouples actin forces from the neck, and that this delays scission. Since invagination lengths of *rvs167a* cells are increased towards WT by overexpression of the BAR domain alone (Fig.3.12A), I propose that localization of Rvs BAR domains to the membrane tube stabilizes the membrane. This allows deep invaginations to grow until actin polymerization produces enough forces to overcome this stabilization and sever the membrane. Stabilization of the membrane tube increases with increasing amounts of BAR domains recruited to the membrane tube (Fig.3.12). The requirement for Rvs scaffolding cannot be removed by reducing turgor pressure (Fig.3.13), suggesting that the function of the scaffold is not to counter turgor pressure.

405

406 Scission efficiency decreases with decreased amounts of Rvs: in diploids, lowering the amount
 407 of Rvs by 20 molecules decreases scission efficiency to about 90% from 97%. This indicates that
 408 a particular coverage of the membrane tube is required for effective scaffolding by BAR domains.
 409 In support of this, in BAR strains, fewer numbers of Rvs are recruited, and scission efficiency is
 410 similarly reduced. At low concentrations of Rvs like in the 1xd cells, it is likely that some membrane
 411 tubes recruit the critical number of Rvs, in which case the invaginations grow to near WT lengths.
 412 Over a certain amount of Rvs, adding more BAR domains does not increase the stability of the
 413 tube: in 4xd, the same amount of actin is recruited before scission as in the 2xd and 1xd strains. If
 414 enough forces are generated at 80nm, why is scission efficiency decreased in *rvs167Δ* compared
 415 to WT? Forces from actin may be at a threshold when the invagination is at 80nm. There could be
 416 enough force to sever the membrane, but not enough to sever reliably. The Rvs scaffold then keeps
 417 the network growing to accumulate enough actin to reliably cause scission. Controlling membrane
 418 tube length could also be a way for the cell to control the size of the vesicles formed, and therefore
 419 the amount of cargo packed into the vesicle.

420 What causes membrane scission?

421 We have tested several scission models that include a major role for the Rvs complex. The seemingly
 422 obvious solution to the scission problem is the action of a dynamin-like GTPase. If loss of the yeast
 423 Dynamin Vps1 prevented or delayed scission, the membrane would continue to invaginate longer
 424 than WT lengths, and Sla1 movements of over 140nm should be observed. Rvs centroid movement
 425 would likely also be affected: a bigger jump inwards could indicate that a longer membrane has
 426 been cut. That neither is seen in the behaviour of coat and scission markers indicates that even if
 427 Vps1 is recruited to endocytic sites, it is not necessary for Rvs localization or function, and is not
 428 necessary for scission. The Inp51, Inp52 data tests the lipid hydrolysis model, in which synaptojanins
 429 hydrolyze PIP2 molecules that are not covered by BAR domains, resulting in a boundary between
 430 hydrolyzed and non- hydrolyzed PIP2. This model predicts that interfacial forces generated at the
 431 lipid boundary causes scission (Liu et al., 2006). Inp51 is not seen in patches at the cellular cortex,
 432 but this could be because protein recruitment is below our detection threshold. Inp52 localizes to
 433 the top of invaginations right before scission, consistent with a role in vesicle formation (Fig.3.7D).
 434 Some predictions of the lipid hydrolysis model are inconsistent with our data, however. First, vesicle
 435 scission is expected to occur at the interphase of the hydrolyzed and non-hydrolyzed lipid. Since the
 436 BAR scaffold covers the membrane tube, this interphase would be at the top of the area covered by
 437 Rvs. Kukulski et al., 2012 have shown that vesicles undergo scission at 1/3 the invagination length
 438 from the base: that is, vesicles generated by the lipid boundary would be smaller than have been
 439 measured. Second, removing forces generated by lipid hydrolysis by deleting synaptojanins should
 440 increase invagination lengths, since scission would be delayed or it would fail without those forces.
 441 Deletion of neither Inp51 nor Inp52 changes the invagination lengths: Sla1 movement does not
 442 increase. That the position of the vesicle formed is also unchanged compared to WT is indicated by
 443 the similar magnitude of the jump into the cytoplasm of the Rvs centroid. There are some changes
 444 in the synaptojanin deletion strains (Fig.3.8). In *inp51Δ* cells, Rvs assembly is slightly slower than
 445 that in WT. Therefore, Inp51 could play a role in Rvs recruitment. In the *inp52Δ* strain, about 12% of
 446 Sla1-GFP tracks retract, indicated that scission fails in those cases. Although this is low compared to
 447 the failed scission rate of *rvs167Δ* cells (close to 30%), this data could suggest a moderate influence
 448 of Inp52 on scission. Rvs centroid persists after scission for about a second longer in *inp52Δ* cells
 449 than in WT, indicating that disassembly of Rvs on the base of the newly formed vesicle is delayed.
 450 Inp52 is likely involved in vesicle un- coating Deletion of synaptojanin-like Inp52 does not affect the
 451 movement of the invagination. In spite of this, Sla1 patches persist for longer after scission in the
 452 *inp52Δ* than in WT cells, as does Rvs167, indicated by the arrows in Fig.3.8A,D. Persistence of both
 453 suggests that rather than the scission timepoint, post-scission disassembly of proteins from the
 454 vesicle is inhibited in *inp52Δ* cells. Inp52 then plays a role in recycling endocytic proteins from the

455 vesicle to the plasma membrane. The slower assembly of Rvs in *inp51Δ* and the increase in coat
456 retraction rates of *inp52Δ* could indicate that there is a slight effect on Rvs recruitment, and that
457 lipid hydrolysis could play a small role in scission.

458

459 Protein-friction mediated membrane scission proposes that BAR domains induce a frictional force
460 on the membrane, causing scission. In Rvs duplicated haploid cells (2xh), adding up to 1.6x the
461 WT (1xh) amount of Rvs to membrane tubes does not affect the length at which the membrane
462 undergoes scission (Fig.3.9). If more BAR domains were added to the membrane tube, frictional
463 force generated as the membrane is pulled under it should increase, and the membrane should
464 rupture faster. That is, membrane scission occurs as soon as WT forces are generated on the tube.
465 Since BAR domains are added at a faster rate in the 2xh cells, these forces would be reached at
466 shorter invagination lengths. In 2xh cells, WT amount of Rvs is recruited at about 1.8 seconds before
467 maximum fluorescent intensity, but scission does not occur at this time. Instead, Rvs continues
468 to accumulate, and the invagination continues to grow. In diploid strains, adding 1.4x the WT
469 amount of Rvs in the 4x Rvs case also does not change length of membrane that undergoes scission.
470 Therefore, protein friction due to Rvs does not appear to contribute significantly to membrane
471 scission in yeast endocytosis.

472 Maximum amount of Abp1 measured in all the diploid strains is about 220 molecules (Fig.3.11).
473 In this case, only one allele of Abp1 is fluorescently tagged, so half the amount of Abp1 recruited
474 is measured. The maximum amount of Abp1 recruited is then double that measured, which is
475 about 440±20 molecules (assuming equal expression and recruitment of tagged and untagged
476 Abp1). In WT haploid cells, the maximum number of Abp1 measured is 460±20 molecules. That the
477 same number of molecules of Abp1 is recruited in all cases before scission indicates that scission
478 timing depends on the amount of Abp1, and hence, on the amount of actin recruited. This data
479 is consistent with actin supplying the forces necessary for membrane scission. The membrane
480 invagination continues until the “right” amount of actin is recruited. At this amount of actin, enough
481 forces are generated to rupture the membrane. The amount of force necessary is determined by
482 the physical properties of the membrane like membrane rigidity, tension, and proteins accumulated
483 on the membrane (Dmitrieff and Needeelec, 2015). Vesicle scission releases membrane-bound Rvs,
484 resulting in release of the SH3 along with BAR domains. Release of the SH3 domains could indicate
485 to its binding partner in the actin network that vesicle scission has occurred, beginning disassembly
486 of actin components. In BAR strains, a low amount of actin is recruited (Fig.3.4C). Although the
487 absence of the SH3 domain severely perturbs the actin network, the mechanistic effect of this
488 perturbation is unclear.

489 **Model for membrane scission**

490 I propose that Rvs is recruited to sites by two distinct mechanisms. SH3 domains cluster Rvs
491 at endocytic sites. This SH3 interaction increases the efficiency with which the BAR domains
492 sense curvature on tubular membranes. BAR domains bind to endocytic sites by sensing tubular
493 membrane. BAR domains are recruited over the entire membrane tube, but do not form a tight
494 helical scaffold. Membrane shape is stabilized against fluctuations that could cause scission by
495 the BAR-membrane interaction. This prevent actin forces from rupturing the membrane, and the
496 invaginations continue to grow in length as actin continues to polymerize. BAR recruitment to
497 membrane tubes is restricted by the surface area of the tube: after a certain amount of Rvs, the
498 excess interacts with endocytic sites via the SH3 domain. Adding over a certain amount of Rvs also
499 does not increase the stabilization effect on the tube. As actin continues to polymerize, at a certain
500 amount of actin, enough forces are generated to overcome the resistance to membrane scission
501 provided by the BAR scaffold. The membrane ruptures, and vesicles are formed. Synaptojanins
502 may help recruit Rvs at endocytic sites: Inp51 and Inp52 have proline rich regions that could act as
503 binding sites for Rvs167 SH3 domains. They are involved in vesicle uncoating post-scission, likely by
504 dephosphorylating PIP2 and inducing disassembly of PIP2-binding endocytic proteins. Eventually

505 phosphorylation regulation allows endocytic proteins to be reused at endocytic sites, while the
506 vesicle is transported elsewhere into the cell.

507 Morbi luctus, wisi viverra faucibus pretium, nibh est placerat odio, nec commodo wisi enim eget
508 quam. Quisque libero justo, consectetur a, feugiat vitae, porttitor eu, libero. Suspendisse sed
509 mauris vitae elit sollicitudin malesuada. Maecenas ultricies eros sit amet ante. Ut venenatis velit.
510 Maecenas sed mi eget dui varius euismod. Phasellus aliquet volutpat odio. Vestibulum ante ipsum
511 primis in faucibus orci luctus et ultrices posuere cubilia Curae; Pellentesque sit amet pede ac sem
512 eleifend consectetur. Nullam elementum, urna vel imperdiet sodales, elit ipsum pharetra ligula,
513 ac pretium ante justo a nulla. Curabitur tristique arcu eu metus. Vestibulum lectus. Proin mauris.
514 Proin eu nunc eu urna hendrerit faucibus. Aliquam auctor, pede consequat laoreet varius, eros
515 tellus scelerisque quam, pellentesque hendrerit ipsum dolor sed augue. Nulla nec lacus.

516 Methods and Materials

517 Guidelines can be included for standard research article sections, such as this one.

518 Nulla malesuada porttitor diam. Donec felis erat, congue non, volutpat at, tincidunt tristique,
519 libero. Vivamus viverra fermentum felis. Donec nonummy pellentesque ante. Phasellus adipiscing
520 semper elit. Proin fermentum massa ac quam. Sed diam turpis, molestie vitae, placerat a, molestie
521 nec, leo. Maecenas lacinia. Nam ipsum ligula, eleifend at, accumsan nec, suscipit a, ipsum.
522 Morbi blandit ligula feugiat magna. Nunc eleifend consequat lorem. Sed lacinia nulla vitae enim.
523 Pellentesque tincidunt purus vel magna. Integer non enim. Praesent euismod nunc eu purus.
524 Donec bibendum quam in tellus. Nullam cursus pulvinar lectus. Donec et mi. Nam vulputate metus
525 eu enim. Vestibulum pellentesque felis eu massa.

526 Citations

527 LaTeX formats citations and references automatically using the bibliography records in your .bib
528 file, which you can edit via the project menu. Use the `\cite` command for an inline citation, like
529 `?`, and the `\citep` command for a citation in parentheses (`?`). The LaTeX template uses a slightly-
530 modified Vancouver bibliography style. If your manuscript is accepted, the eLife production team
531 will re-format the references into the final published form. *It is not necessary to attempt to format*
532 *the reference list yourself to mirror the final published form.* Please also remember to **delete the line**
533 `\nocite{*}` in the template just before `\bibliography{...}`; otherwise *all* entries from your .bib
534 file will be listed!

535 Acknowledgments

536 Additional information can be given in the template, such as to not include funder information in
537 the acknowledgments section.

538 References

- 539 Bitsikas, V., Corrêa, I. R., and Nichols, B. J. (2014). Clathrin-independent pathways do not contribute significantly
540 to endocytic flux. *eLife*, 3:e03970.
- 541 Bui, H. T., Karren, M. A., Bhar, D., and Shaw, J. M. (2012). A novel motif in the yeast mitochondrial dynamin Dnm1
542 is essential for adaptor binding and membrane recruitment. *The Journal of cell biology*, 199(4):613–22.
- 543 Cestra, G., Castagnoli, L., Dente, L., Minenkova, O., Petrelli, A., Migone, N., Hoffmüller, U., Schneider-Mergener, J.,
544 and Cesareni, G. (1999). The SH3 domains of endophilin and amphiphysin bind to the proline-rich region of
545 synaptojanin 1 at distinct sites that display an unconventional binding specificity. *The Journal of biological*
546 *chemistry*, 274(45):32001–7.
- 547 Colwill, K., Field, D., Moore, L., Friesen, J., and Andrews, B. (1999). In Vivo Analysis of the Domains of Yeast Rvs167p
548 Suggests Rvs167p Function Is Mediated Through Multiple Protein Interactions. *Genetics*, 152(3):881–893.
- 549 D'Hondt, K., Heese-Peck, A., and Riezman, H. (2000). Protein and Lipid Requirements for Endocytosis. *Annual*
550 *Review of Genetics*, 34(1):255–295.

551 Farsad, K., Ringstad, N., Takei, K., Floyd, S. R., Rose, K., and De Camilli, P. (2001). Generation of high curvature
552 membranes mediated by direct endophilin bilayer interactions. *The Journal of Cell Biology*, 155(2):193–200.

553 Ferguson, S. M., Brasnjo, G., Hayashi, M., Wölfel, M., Collesi, C., Giovedi, S., Raimondi, A., Gong, L. W., Ariel, P.,
554 Paradise, S., O'Toole, E., Flavell, R., Cremona, O., Miesenböck, G., Ryan, T. A., and De Camilli, P. (2007). A selective
555 activity-dependent requirement for dynamin 1 in synaptic vesicle endocytosis. *Science*, 316(5824):570–574.

556 Ferguson, S. M., Raimondi, A., Paradise, S., Shen, H., Mesaki, K., Ferguson, A., Destaing, O., Ko, G., Takasaki, J.,
557 Cremona, O., O'Toole, E., and De Camilli, P. (2009). Coordinated actions of actin and BAR proteins upstream
558 of dynamin at endocytic clathrin-coated pits. *Developmental cell*, 17(6):811–822.

559 Friesen, H., Humphries, C., Ho, Y., Schub, O., Colwill, K., and Andrews, B. (2006). Characterization of the Yeast
560 Amphiphysins Rvs161p and Rvs167p Reveals Roles for the Rvs Heterodimer In Vivo. *Molecular Biology of the*
561 *Cell*, 17(3):1306–1321.

562 Galli, V., Sebastian, R., Moutel, S., Ecard, J., Perez, F., and Roux, A. (2017). Uncoupling of dynamin polymerization
563 and GTPase activity revealed by the conformation-specific nanobody dynab. *eLife*, 6:e25197.

564 Goud Gadila, S. K., Williams, M., Saimani, U., Delgado Cruz, M., Makaraci, P., Woodman, S., Short, J. C., McDermott,
565 H., and Kim, K. (2017). Yeast dynamin Vps1 associates with clathrin to facilitate vesicular trafficking and
566 controls Golgi homeostasis. *European Journal of Cell Biology*, 96(2):182–197.

567 Grabs, D., Slepnev, V. I., Songyang, Z., David, C., Lynch, M., Cantley, L. C., and De Camilli, P. (1997). The SH3
568 domain of amphiphysin binds the proline-rich domain of dynamin at a single site that defines a new SH3
569 binding consensus sequence. *The Journal of biological chemistry*, 272(20):13419–25.

570 Grigliatti, T. A., Hall, L., Rosenbluth, R., and Suzuki, D. T. (1973). Temperature-Sensitive Mutations in *Drosophila*
571 *melanogaster* XIV. A Selection of Immobile Adults *. *Molec. gen. Genet*, 120:107–114.

572 Hoepfner, D., van den Berg, M., Philippsen, P., Tabak, H. F., and Hettema, E. H. (2001). A role for Vps1p, actin, and
573 the Myo2p motor in peroxisome abundance and inheritance in *Saccharomyces cerevisiae*. *The Journal*
574 *of Cell Biology*, 155(6):979–990.

575 Kaksonen, M. and Roux, A. (2018). Mechanisms of clathrin-mediated endocytosis.

576 Kaksonen, M., Sun, Y., and Drubin, D. G. (2003). A pathway for association of receptors, adaptors, and actin
577 during endocytic internalization. *Cell*, 115(4):475–487.

578 Kaksonen, M., Toret, C. P., and Drubin, D. G. (2005). A modular design for the clathrin- and actin-mediated
579 endocytosis machinery. *Cell*, 123(2):305–320.

580 Kishimoto, T., Sun, Y., Buser, C., Liu, J., Michelot, A., and Drubin, D. G. (2011). Determinants of endocytic
581 membrane geometry, stability, and scission. *Proceedings of the National Academy of Sciences of the United*
582 *States of America*, 108(44):E979–E988.

583 Kübler, E., Riezman, H., Riezman, H., and Riezman, H. (1993). Actin and fimbrin are required for the internalization
584 step of endocytosis in yeast. *The EMBO journal*, 12(7):2855–62.

585 Kukulski, W., Schorb, M., Kaksonen, M., and Briggs, J. G. (2012). Plasma Membrane Reshaping during Endocytosis
586 Is Revealed by Time-Resolved Electron Tomography. *Cell*, 150(3):508–520.

587 Lila, T. and Drubin, D. G. (1997). Evidence for physical and functional interactions among two *Saccharomyces*
588 *cerevisiae* SH3 domain proteins, an adenyl cyclase-associated protein and the actin cytoskeleton. *Molecular*
589 *Biology of the Cell*, 8(2):367–385.

590 Liu, J., Sun, Y., Drubin, D. G., and Oster, G. F. (2009). The Mechanochemistry of Endocytosis. *PLoS Biol*,
591 7(9):e1000204.

592 Madania, A., Dumoulin, P., Grava, S., Kitamoto, H., Scharer-Brodbeck, C., Soulard, A., Moreau, V., and Winsor,
593 B. (1999). The *Saccharomyces cerevisiae* Homologue of Human Wiskott-Aldrich Syndrome Protein Las17p
594 Interacts with the Arp2/3 Complex. *Molecular Biology of the Cell*, 10(10):3521–3538.

595 Meinecke, M., Boucrot, E., Camdere, G., Hon, W.-C., Mittal, R., and McMahon, H. T. (2013). Cooperative recruitment
596 of dynamin and BIN/amphiphysin/Rvs (BAR) domain-containing proteins leads to GTP-dependent membrane
597 scission. *The Journal of biological chemistry*, 288(9):6651–61.

598 Moustaq, L., Smaczynska-de Rooij, I. I., Palmer, S. E., Marklew, C. J., and Ayscough, K. R. (2016). Insights into
599 dynamin-associated disorders through analysis of equivalent mutations in the yeast dynamin Vps1. *Microbial*
600 *cell (Graz, Austria)*, 3(4):147–158.

601 Munn, A. L., Stevenson, B. J., Geli, M. I., and Riezman, H. (1995). end5, end6, and end7: Mutations that cause
602 actin delocalization and block the internalization step of endocytosis in *Saccharomyces cerevisiae*. *Molecular*
603 *Biology of the Cell*, 6(12):1721–1742.

604 Nannapaneni, S., Wang, D., Jain, S., Schroeder, B., Highfill, C., Reustle, L., Pittsley, D., Maysent, A., Moulder, S.,
605 McDowell, R., and Kim, K. (2010). The yeast dynamin-like protein Vps1: vps1 mutations perturb the internal-
606 ization and the motility of endocytic vesicles and endosomes via disorganization of the actin cytoskeleton.
607 *European Journal of Cell Biology*, 89(7):499–508.

608 Peters, C., Baars, T. L., Bühler, S., and Mayer, A. (2004). Mutual control of membrane fission and fusion proteins.
609 *Cell*, 119(5):667–78.

610 Picco, A., Mund, M., Ries, J., Nédélec, F., and Kaksonen, M. (2015). Visualizing the functional architecture of the
611 endocytic machinery. *eLife*, page e04535.

612 Rooij, I. I. S.-d., Allwood, E. G., Aghamohammadzadeh, S., Hettema, E. H., Goldberg, M. W., and Ayscough,
613 K. R. (2010). A role for the dynamin-like protein Vps1 during endocytosis in yeast. *Journal of Cell Science*,
614 123(20):3496–3506.

615 Rothman, J. H., Raymond, C. K., Gilbert, T., O'Hara, P. J., and Stevens, T. H. (1990). A putative GTP binding protein
616 homologous to interferon-inducible Mx proteins performs an essential function in yeast protein sorting. *Cell*,
617 61(6):1063–1074.

618 Shupliakov, O., Löw, P., Grabs, D., Gad, H., Chen, H., David, C., Takei, K., De Camilli, P., and Brodin, L. (1997).
619 Synaptic vesicle endocytosis impaired by disruption of dynamin-SH3 domain interactions. *Science (New York,*
620 *N.Y.)*, 276(5310):259–63.

621 Sivadon, P., Crouzet, M., and Aigle, M. (1997). Functional assessment of the yeast Rvs161 and Rvs167 protein
622 domains. *FEBS letters*, 417(1):21–27.

623 Smaczynska-de Rooij, I. I., Allwood, E. G., Mishra, R., Booth, W. I., Aghamohammadzadeh, S., Goldberg, M. W., and
624 Ayscough, K. R. (2012). Yeast Dynamin Vps1 and Amphiphysin Rvs167 Function Together During Endocytosis.
625 *Traffic*, 13(2):317–328.

626 Sweitzer, S. M. and Hinshaw, J. E. (1998). Dynamin Undergoes a GTP-Dependent Conformational Change Causing
627 Vesiculation. *Cell*, 93(6):1021–1029.

628 Takei, K., McPherson, P. S., Schmid, S. L., and Camilli, P. D. (1995). Tubular membrane invaginations coated by
629 dynamin rings are induced by GTP- γ S in nerve terminals. *Nature*, 374(6518):186–190.

630 Youn, J.-Y., Friesen, H., Kishimoto, T., Henne, W. M., Kurat, C. F., Ye, W., Ceccarelli, D. F., Sicheri, F., Kohlwein, S. D.,
631 McMahon, H. T., and Andrews, B. J. (2010). Dissecting BAR Domain Function in the Yeast Amphiphysins Rvs161
632 and Rvs167 during Endocytosis. *Molecular Biology of the Cell*, 21(17):3054–3069.

633 Yu, X. and Cai, M. (2004). The yeast dynamin-related GTPase Vps1p functions in the organization of the actin
634 cytoskeleton via interaction with Sla1p. *Journal of Cell Science*, 117(17):3839–3853.

635 Zhang, P. and Hinshaw, J. E. (2001). Three-dimensional reconstruction of dynamin in the constricted state. *Nature*
636 *Cell Biology*, 3(10):922–926.

637 Zhao, W.-D., Hamid, E., Shin, W., Wen, P. J., Krystofiak, E. S., Villarreal, S. A., Chiang, H.-C., Kachar, B., and Wu, L.-G.
638 (2016). Hemi-fused structure mediates and controls fusion and fission in live cells. *Nature*, 534(7608):548–52.